Organic Electronics

DOI: 10.1002/anie.200905117

Strain and Hückel Aromaticity: Driving Forces for a Promising New Generation of Electron Acceptors in Organic Electronics**

*F. G. Brunetti, X. Gong, M. Tong, A. J. Heeger, and Fred Wudl**

The tangible possibility of fabricating flexible, lightweight organic photovoltaic devices (OPVs) by using roll-to-roll coaters, similar to those used in the production of print magazines and newspapers, renders this technology a valid alternative to expensive crystalline silicon photovoltaic cells.[1–3] The most widely used active layer for these OPVs, the so-called bulk heterojunction (BHJ),[4,5] is based on photoinduced charge transfer from an electron-donating material, such as a light-absorbing and hole-conducting polymer, to an electron-accepting component, typically fullerene [60] and its derivative 1-(3-methoxycarbonyl) propyl-1-phenyl-[6,6]-C_{61} ([C_{60}]PCBM).[6,7]

Several research groups have reported a wide range of new polymeric donor structures that absorb light over a broad wavelength range, and have a narrow energy gap and increased charge transport and collection at the electrode. However, there have been fewer reports on new structures of acceptor components that do not contain fullerene derivatives.[8–11] C_{60} and C_{70} PCBMs are currently considered the most successful acceptor architectures, despite only slight improvements when modifying these functionalized fullerenes.[12–14] For example, the insertion of electron-donating groups on the phenyl ring of the [C_{60}]PCBM to tune the lowest unoccupied molecular orbital (LUMO) energy levels improved the open-circuit voltage (V_{oc}), while maintaining a relatively unchanged efficiency.[15] Furthermore, [C_{70}]PCBM, which absorbs a wider range of wavelengths than [C_{60}]PCBM,[16] was employed with low-band-gap polymers such as poly[2,6-(4,4-bis-(2-ethylhexyl-4H-cyclopenta[2,1-b;3,4b′]-dithiophene)-alt-4,7-(2,1,3-benzothiadizole)] (PCPDTBT), to broaden the photocurrent spectral range. Although encouraging photocurrent and photovoltage values were obtained, a low overall efficiency, which arises from loss mechanisms, was observed.[17] Despite the wide use of these fullerene derivatives, the synthesis of new acceptors with energy levels significantly different from those of current C_{60} derivatives, and wide versatility in terms of derivatization and functionalization is urgently required. Herein, we report the inherent potential of a new generation of acceptor compounds based on the 9,9′-bifluorenylidene[18] (99′BF) backbone. 99′BF could be considered a tetrabenzofulvalene with an atom numbering that reflects fluorene linked by a double bond between the 9 and 9′ carbon atoms. In the ground state, 99′BF is forced to be coplanar because of the presence of the double bond, but the repulsive interaction between the H1–H1′ and H8–H8′ protons twists the structure of the dimer.[19–21] The addition of one electron across the C9–C9′ bond is highly favorable for two main reasons: steric (“twist”)[22] strain relief and gain in aromaticity to a 14-π-electron system[23] (Scheme 1).

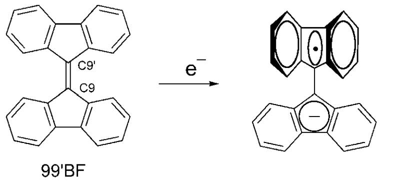

Scheme 1. Formation of 99′BF 14-π-electron fluorenide anion after the addition of one electron across the C9–C9′ double bond.

A further advantage is that the corresponding fluorene radical, which was isolated and characterized by electrochemical and ESR studies, is stable under certain conditions.[24–26] In addition, 99′BF is a much more versatile scaffold than the fullerenes as, theoretically, it has twelve different sites for functionalization by substitution. On the other hand, buckminsterfullerene can only be functionalized by addition reactions, which result in a major modification of the electronic structure with each subsequent addition.[27,28] Based on this reasoning, we synthesized and characterized a series of overcrowded polycycles (Scheme 2), and some very preliminary BHJ solar cells are briefly presented.

Compound **6d**, which was functionalized with donor substituents, was obtained from a one-pot reaction by treating 2,7-dimethoxy-9-fluorenone[29] **7** in the presence of Lawesson’s reagent in toluene at reflux (Scheme 3). We hypothesized that the formation of the corresponding thione would occur first, followed by dimerization via a carbene, in accordance with the mechanism proposed by Agranat and co-workers[30] for compound **5**. The analogous isomer **1**, with methoxy groups at positions 3 and 6 instead of 2 and 7, was prepared by dimerization of the corresponding 3,6-dime-

---

[*] Dr. F. G. Brunetti, Prof. F. Wudl
Materials Research Laboratory
University of California Department of Chemistry and Biochemistry
Santa Barbara, CA 93106 (USA)
Fax: (+1) 805-893-4120
E-mail: wudl@chem.ucsb.edu

Dr. F. G. Brunetti, Dr. X. Gong, Dr. M. Tong, Prof. A. J. Heeger, Prof. F. Wudl
Center for Polymers and Organic Solids, University of California
Santa Barbara, CA 93106 (USA)

[**] We are grateful to The University of California, Santa Barbara MRL for financial support through seed project N4SEWF and to Konanka Technologies Inc. Technical assistance from Dr. J. Pavlovich for the mass spectroscopy and G. Wu for the crystal structure is also acknowledged.

Supporting information for this article is available on the WWW under http://dx.doi.org/10.1002/anie.200905117.

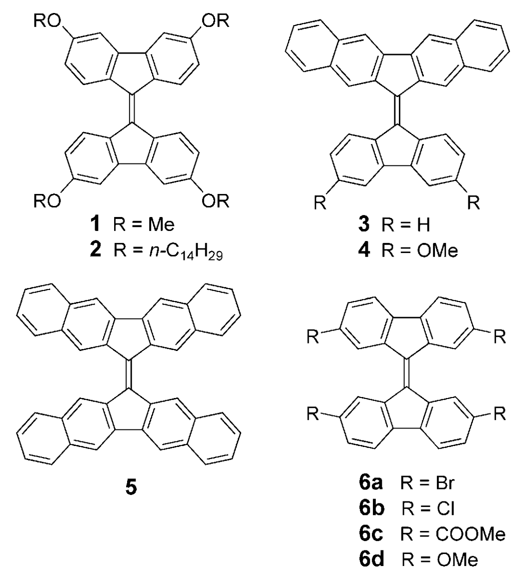

Scheme 2. Structures of overcrowded polycycles.

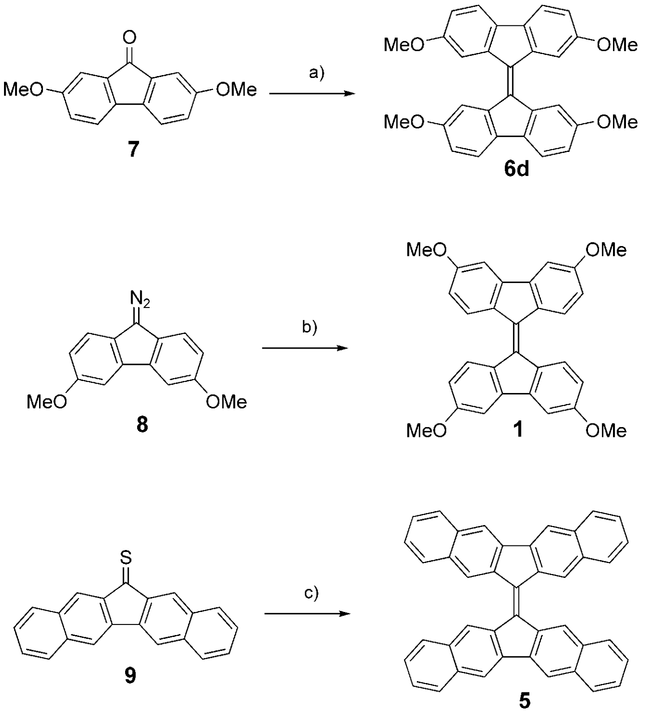

Scheme 3. a) Lawesson's reagent, toluene, reflux, 50%; b) CuBr, THF, reflux, 70%; c) Cu powder (1 equiv), toluene, reflux, 60%.

thoxy-9-diazofluorene[31] **8** using a catalytic amount of CuBr (70% yield). The synthesis of **5** was carried out following the reported procedure,[30] but with a slight modification: the presence of copper powder as the metal catalyst reduced the reaction time from 8 days to only a few hours. We also designed two asymmetric compounds (**3** and **4**) to introduce asymmetry for higher solubility and more conjugation in one unit of the fulvalene. Thus, **3** and **4** were prepared by applying Barton's two-fold extrusion diazo–thione coupling method (Scheme 4).[32,33] Thione **9** was coupled with the corresponding diazofluorene **8** and **10** in THF and stirred overnight (yield 60%). Formation of the dissymmetric dimers **3** and **4** was accompanied by a small amount of the corresponding symmetric benzofulvalene derivatives, thus lowering the yield of the target molecules.

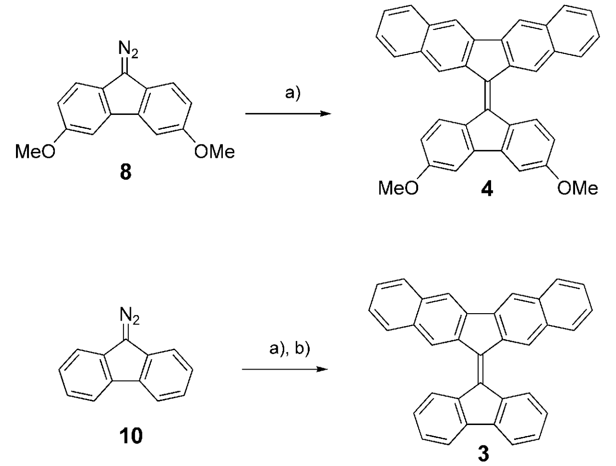

Scheme 4. a) Compound **9**, THF, RT; b) Cu metal, toluene, reflux, 60%.

Compound **4**, which was recrystallized from acetonitrile, formed deep red needles, whose structure and packing is shown in Figure 1. An edge-to-face π–π stacking motif was observed in the solid state, along with a minimal intermolecular distance of 3.61 Å between the dibenzofluorenylidene fragment and the 3,6-dimethoxyfluorene unit of a neighboring molecule, probably because of the asymmetry of the molecule and the electron density difference of each fragment. Importantly, the solid-state interactions in this arrangement could facilitate the intermolecular delocalization of the negative charge during the migration to the electrode.

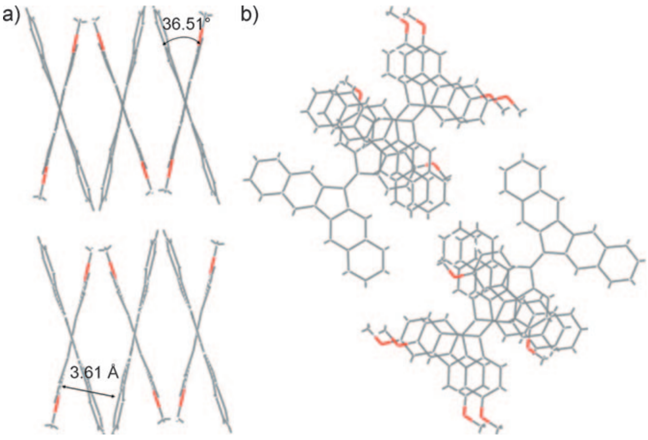

Figure 1. a) Torsional angle and b) π-stacking motif of **4**.

As in the crystal structure of 99′BF,[19–20] X-ray diffraction studies reveal that **4** is significantly distorted from planarity with a torsional angle of 36.51°, in contrast to 39.3° for the parent compound. This difference can be attributed to the presence of donor groups that increase the length of the double bond between C9 and C9′ from 1.364 Å for 99′BF to

1.382 Å, and consequently decrease the repulsive interaction between the neighboring protons.

Long alkoxy chains were inserted into the 99′BF nucleus to further enhance solubility, raise the LUMO, and reduce crystallinity. The synthesis of dimer **2**, which was carried out by following the same procedure as dimer **1**, started with 3,6-dihydroxy-9-fluorenone and proceeded via a diazo intermediate (see the Supporting Information for details).

Contrary to the dimers described previously, the presence of electron-withdrawing functionalities in **6a**–**c** dramatically reduced their solubility in common organic solvents. A similar observation was reported by Angeloni et al.[34] for a 99′BF tetracarbonitrile. Compounds **6a**–**c** were obtained in 50–70 % yields by dimerization of the corresponding substituted 9-bromofluorenes in the presence of DBU as organic base (see the Supporting Information for details). Figure 2 shows the optical absorption of compounds **1**, **4**, **5**, 99′BF, and C_{60} and C_{70} PCBMs for comparison. The absorption of **5**, which is the largest of this set of compounds, is shifted to longer wavelengths by approximately 90 nm from that of the parent compound 99′BF because of the enhanced π-electron delocalization. The absorption of these dimers, which is centered in the range 400–600 nm, is much higher than that of $[C_{60}]$PCBM and almost comparable with that of $[C_{70}]$PCBM ($\lambda_{onset} \approx 710$ nm)[16] in the same range of wavelengths.

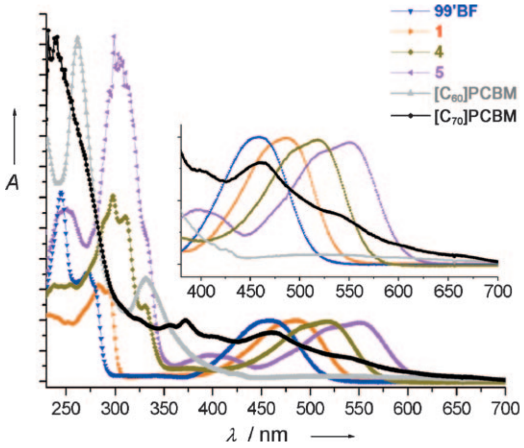

Figure 2. UV/Vis absorption spectra of compounds **1** (orange), **4** (dark yellow), **5** (magenta), 99′BF (blue), and $[C_{60}]$- and $[C_{70}]$PCBMs (gray and black respectively).

However, the absorption maxima for compounds **3** and **4** are significantly red-shifted from that of 99′BF; these results reveal how the effect of the enhanced conjugation of one fragment dominates the presence of the methoxy groups in the remaining part of the molecule. Regardless of the alkoxy chain length, compounds **1** and **2** show an optical absorption centered around 485 nm and 497 nm, respectively. These absorptions are red-shifted by approximately 30 nm from the unsubstituted 99′BF, and arise from the donating effect of the substituents. UV/Vis spectra of solutions of **6a**–**c** and **6d** show an optical absorption centered around 458 nm as in the parent compound, thus indicating no effect of any substituents at positions 2,2′,7,7′ on the optical absorption.

Similar overcrowded alkenes described by Feringa et al. show only a slight red shift after the introduction of electron-donating or electron-withdrawing groups as for dimers **6**, while the bathochromic shift of 20–60 nm was observed after photochemical isomerization, probably because of steric hindrance in the fjord region.[35]

Optical band gaps determined from the onset of absorption were found to be consistent with those measured by electrochemistry (see below), but differed by as much as 0.38 eV. Energy levels, which were determined by electrochemical analysis, and optical values are summarized in Table 1. Except for **6a**–**c**, all the dimers showed quasi-reversible reduction and oxidation waves. In general, the first reduction wave can be attributed to the formation of the radical anion and the second to the corresponding dianion.[26] Specifically, the location of the LUMO of **2** is influenced by the inductive effect of the alkoxy groups, and reaches a value of −3.09 eV. We also observed a narrowing of the HOMO–LUMO gap (HOMO = highest occupied molecular orbital) in **4** and **5** because of the extension of the π-conjugated system with an E_g value as small as 1.90 eV. It should be noted that the orbital energy levels of the HOMO (5.06–5.58 eV) and LUMO (3.09–3.39 eV), are accessible to a large number of conjugated polymers. By employing donors that also have a relatively high LUMO level, such as *rr*-poly(3-hexylthiophene) (*rr*-P3HT; −3.0 eV), we estimate an V_{oc} value above 1 eV, which is higher than that of $[C_{60}]$PCBM and its derivative (bisPCBM),[36] and a LUMO–LUMO gap between 99′BF dimers and selective donor polymers that would still allow an efficient photon-to-charge conversion.[37–40]

Table 1: Optical and electrochemical data.

Dimer	λ_{max} [nm][a]	λ_{onset} [nm][b]	HOMO [eV][c]	LUMO [eV][c]	$E_{g,CV}$ [eV][d]	$E_{g,optical}$ [eV][e]
99′BF	458	513	−5.58	−3.37	2.22	2.42
1	485	536	−5.11	−3.11	2.00	2.31
2	497	542	−5.06	−3.09	1.97	2.29
3	504	560	−5.41	−3.36	2.06	2.21
4	517	569	−5.17	−3.24	1.94	2.18
5	546	603	−5.25	−3.35	1.90	2.05
6d	460	520	−5.38	−3.39	1.99	2.38
6a	458	516	–	−3.7	–	2.40
6b	458	515	–	−3.7	–	2.41
6c	460	513	–	−3.7	–	2.42

[a] Maximum absorption of the long wavelength feature. [b] The intercept of the slope of the absorption tail and the minimum absorption. [c] Calculated by measuring the difference between the onsets of oxidation and reduction and the half-wave potential of the ferrocene standard. [d] Determined from the onsets of the first reduction and oxidation. [e] Calculated from λ_{onset}.

The thermal behavior of compounds **1**–**5** was determined by thermogravimetric analysis (TGA) and differential scanning calorimetry (DSC). TGA analyses show that all compounds have a relatively high decomposition temperature (T_d), at least 260 °C and up to 400 °C, with a weight loss within a range of 4–5 % (Table 2). These data clearly indicate good thermal stability, which is one of the basic requirements for a long lifetime in organic devices.

Table 2: Thermal properties of dimers.

Dimer	1	2	3	4	5
T_{deg} [°C][a]	234	340	230	240	388
T_m [°C][b]	210	65	230	186	380

[a] Degradation temperature observed from TGA (4–5 % weight loss at 10 °C min^{-1}). [b] Melting temperature observed from DSC (at 5 °C min^{-1}).

The thermal transitions were studied by DSC and are also reported in Table 2. Each compound exhibited a melting point (T_m) close to the T_d value, except for **2**, which showed a glass transition around 65 °C, because of the presence of long alkyl chains that render this particular dimer more amorphous than crystalline.

To estimate the electron-accepting capability and to prove the predicted value of the open-circuit voltage (V_{oc}), polymer solar cells were fabricated using the dissymmetric fulvalene benzologue **4** as acceptor and P3HT as the donor component. Two architectures, ITO/PEDOT/P3HT:**4**/Al and ITO/PEDOT/P3HT:**4**/Ba/Al (ITO = indium tin oxide, PEDOT = poly(3,4-ethylenedioxythiophene)), were studied, in which either an Al or Ba/Al cathode was employed. The voltage–current (*J*–*V*) characteristics of both BHJ devices under AM1.5G simulated illumination (100 mW cm^{-2} irradiation intensity) are shown in Figure 3. Interestingly, an open-circuit voltage (V_{oc}) of 1.10 V, which is almost double that of [C_{60}]PCBM, a fill factor (*FF*) of 0.40, and a power conversion efficiency (PCE) of 1.7 % were achieved by employing barium as the cathode.

In conclusion, we studied the versatility of the 99′BF core as a function of substitution and the extension of the π-conjugated system. These overcrowded polycycles were successfully obtained in high yields, and use of an expensive metal catalyst or lengthy synthetic routes were avoided. The electronic and optical properties of the polycycles were easily tuned after functionalization, thus demonstrating an interesting flexibility of these electron acceptor materials. In terms of OPV devices, a V_{oc} value of 1.10 eV, which is essentially double that of [60]PCBM, a fill factor of 0.40, and an efficiency of around 2 % was achieved. A detailed description of the optoelectronic properties of these dimers combined with specific donor polymers is under investigation.[40]

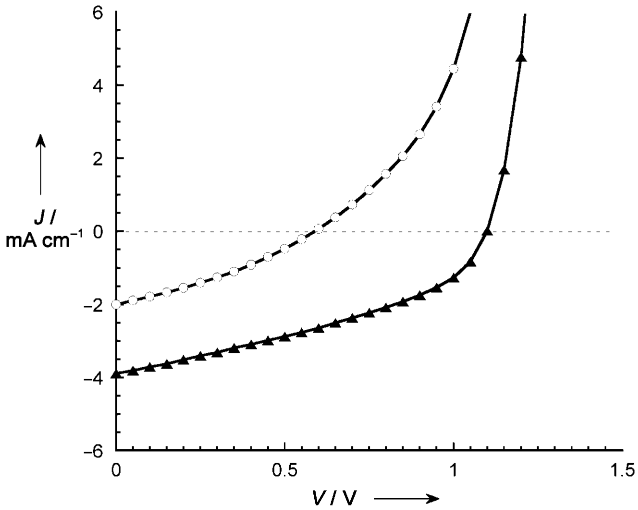

Figure 3. Current–voltage characteristics of dimer 4:P3HT devices (1:1.5 weight ratio) under AM 1.5G illumination using Al (circles) and Ba/Al (triangles) cathodes.[40]

Experimental Section

Chemicals were purchased from Sigma–Aldrich or Acros Organics and used as received without further purification. All dry solvents were freshly distilled under argon over an appropriate drying agent prior to use. ^{1}H and ^{13}C NMR spectra were obtained on a Varian Unity Inova 500 MHz spectrometer and referenced to the solvent peak. Mass spectrometry was performed by the UC Santa Barbara Mass Spectrometry Laboratory. UV/Vis spectra were recorded on a Agilent 8453 spectrophotometer using DCM solutions of the dimers in 1 cm quartz cuvettes at room temperature. The spectrum of each dimer was then normalized to its maximum absorption (typically ca. 450–550 nm). The electrochemical measurements were carried out with a Princeton Applied Research Model 263 A Potentiostat/Galvanostat employing Ag/AgCl as reference electrode, a platinum wire as a counterelectrode, and an internal ferrocene/ferrocenium standard. Solution of 99′BF derivatives were 1 mg mL^{-1}, except **6a–c** 0.5 mg mL^{-1}, in dry DCM containing 0.1 M tetrabutylammonium hexafluorophosphate as the supporting electrolyte. The thermogravimetric and calorimetric analyses were performed with a TGA Q50 (TA Instruments) at 10 °C min^{-1} under N_2 and DSC Q10 (TA Instrument) at the heating rate of 5 °C min^{-1}. Synthetic details for compounds **1–5** and **6a–d** are described in the Supporting Information. CCDC 753925 contains the supplementary crystallographic data for this paper. These data can be obtained free of charge from The Cambridge Crystallographic Data Centre via www.ccdc.cam.ac.uk/data_request/cif..

Received: September 12, 2009
Revised: November 11, 2009

Keywords: dimerization · electron acceptors · organic electronics · polycycles · solar cells

---

[1] K. M. Coakley, M. D. McGehee, *Chem. Mater.* **2004**, *16*, 4533–4542.
[2] C. J. Brabec, N. S. Sariciftci, J. C. Hummelen, *Adv. Funct. Mater.* **2001**, *11*, 15–26.
[3] G. Li, V. Shrotriya, J. Huang, Y. Yao, T. Moriarty, K. Emery, Y. Yang, *Nat. Mater.* **2005**, *4*, 864–868.
[4] N. S. Sariciftci, L. Smilowitz, J. A. Hegeer, F. Wudl, *Science* **1992**, *258*, 1474–1476.
[5] G. Yu, J. A. Heeger, *J. Appl. Phys.* **1995**, *78*, 4510–4515.
[6] J. C. Hummelen, B. W. Knight, F. LePeq, F. Wudl, J. Yao, C. L. Wilkins, *J. Org. Chem.* **1995**, *60*, 532–538.
[7] G. Yu, J. Gao, J. C. Hummelen, F. Wudl, A. J. Hegeer, *Science* **1995**, *270*, 1789–1791.
[8] G. Dennler, M. C. Scharber, C. J. Brabec, *Adv. Mater.* **2009**, *21*, 1323–1338.
[9] C. P. Chen, S. H. Chan, T. C. Chao, C. Ting, B. T. Ko, *J. Am. Chem. Soc.* **2008**, *130*, 12828–13833.
[10] S. Günes, H. Neugebauer, N. S. Sariciftci, *Chem. Rev.* **2007**, *107*, 1324–1338.
[11] E. Bundgaard, F. C. Krebs, *Sol. Energy Mater. Sol. Cells* **2007**, *91*, 954–985.
[12] M. M. Wienk, M. Turbiez, J. Gilot, R. A. J. Janssen, *Adv. Mater.* **2008**, *20*, 2556–2560.

[13] S. A. Backer, K. Sivula, D. F. Kavulak, J. M. J. Fréchet, *Chem. Mater.* **2007**, *19*, 2927 – 2929.

[14] M. Lenes, S. W. Shelton, A. B. Sieval, D. F. Kronholm, J. C. Hummelen, P. W. M. Blom, *Adv. Funct. Mater.* **2009**, *19*, 3002 – 3007.

[15] F. B. Kooistra, J. Knol, F. Kastenberg, L. M. Popescu, W. J. H. Verhees, J. M. Kroon, J. C. Hummelen, *Org. Lett.* **2007**, *9*, 551 – 554.

[16] F. B. Kooistra, V. D. Mihailetchi, L. M. Popescu, D. Kronholm, P. W. M. Blom, J. C. Hummelen, *Chem. Mater.* **2006**, *18*, 3068 – 3073.

[17] D. Mühlbacher, M. Scharber, M. Morana, Z. G. Zhu, D. Waller, R. Gaudiana, C. Brabec, *Adv. Mater.* **2006**, *18*, 2884 – 2889.

[18] a) P. U. Biedermann, J. J. Stezowski, I. Agranat, *Eur. J. Org. Chem.* **2001**, 15 – 34; b) Although bifluorenylidene should be considered an electron acceptor, it forms a weak charge-transfer complex with tetracyanoquinodimethane (TCNQ). L. Angeloni, G. Sbrana, *J. Raman Spectrosc.* **1983**, *14*, 380 – 385.

[19] J. S. Lee, S. C. Nyburg, *Acta Crystallogr. Sect. C* **1985**, *41*, 560 – 567.

[20] M. Riklin, A. von Zelewsky, A. Bashall, M. McPartlin, A. Baysal, J. A. Connor, J. D. Wallis, *Helv. Chim. Acta* **1999**, *82*, 1666 – 1680.

[21] S. Pogodin, I. Agranat, *J. Org. Chem.* **2002**, *67*, 265 – 270.

[22] M. Rabinovitz, I. Agranat, A. Weitzen-Dagan, *Tetrahedron Lett.* **1974**, *15*, 1241 – 1244.

[23] Y. Cohen, J. Klein, M. Rabinovitz, *J. Chem. Soc. Chem. Commun.* **1986**, 1071 – 1073.

[24] B. J. Tabner, T. Walker, *J. Chem. Soc. Perkin Trans. 2* **1972**, 445 – 449.

[25] E. J. Rothwell, B. J. Tabner, *J. Chem. Soc. Perkin Trans. 2* **1981**, 1384 – 1391.

[26] M. Otero, E. Roman, E. Samuel, D. Gourier, *J. Electroanal. Chem.* **1992**, *325*, 143 – 152.

[27] A. Hirsch, M. Brettreich in *Fullerenes: Chemistry and Reactions*, *Vol. 17*, Wiley-VCH, Weinheim, **2004**.

[28] F. Wudl, *Acc. Chem. Res.* **1992**, *25*, 157 – 161.

[29] J. R. Epperson, M. A. Bruce, J. D. Catt, J. A. Deskus, D. B. Hodges, G. N. Karageorge, D. J. Keavy, C. D. Mahle, R. J. Mattson, A. A. Ortiz, M. F. Parker, K. F. Takaki, B. T. Watson, J. P. Yevich, *Bioorg. Med. Chem.* **2004**, *12*, 4601 – 4611.

[30] A. Levy, M. Goldschmidt, I. Agranat, *Lett. Org. Chem.* **2006**, *3*, 579 – 584.

[31] C. Chuang, S. C. Lapin, A. K. Schrock, G. B. Schuster, *J. Am. Chem. Soc.* **1985**, *107*, 4238 – 4243.

[32] D. H. R. Barton, B. J. Willis, *J. Chem. Soc. Perkin Trans. 1* **1972**, 305 – 310.

[33] D. H. R. Barton, F. S. Guziec, I. Shahak, *J. Chem. Soc. Perkin Trans. 1* **1974**, 1794 – 1799.

[34] G. Sbrana, M. Scotton, L. Angeloni, *J. Chem. Soc. Perkin Trans. 2* **1982**, 1611 – 1614.

[35] B. L. Feringa, R. A. van Delden, N. Koumura, E. M. Geertsema, *Chem. Rev.* **2000**, *100*, 1789 – 1816.

[36] M. Lenes, G. J. A. H. Wetzelaer, F. B. Kooistra, S. C. Veenstra, J. C. Hummelen, P. W. M. Blom, *Adv. Mater.* **2008**, *20*, 2116 – 2119.

[37] W. Ma, C. Yang, X. Gong, K. Lee, A. J. Heeger, *Adv. Funct. Mater.* **2005**, *15*, 1617 – 1622.

[38] A. Gadisa, M. Svensson, M. R. Andersson, O. Inganäs, *Appl. Phys. Lett.* **2004**, *84*, 1609 – 1611.

[39] C. J. Brabec, A. Cravino, D. Meissner, N. S. Sariciftci, M. T. Rispens, L. Sanchez, J. C. Hummelen, T. Fromherz, *Thin Solid Films* **2002**, *403*, 368 – 372.

[40] X. Gong, M. Tong, F. G. Brunetti, D. Moses, F. Wudl, A. J. Heeger, **2009**, unpublished results.